IN VITRO CORROSION RESISTANCE OF A SUPERFERRITIC STAINLESS STEEL IN HANK'S SOLUTION

Sérgio Luiz de Assis
IPEN/CNEN-SP, Av. Prof. Lineu Prestes, 2242, CEP 05508-900, São Paulo, SP – slassis@ipen.br

Sizue Ota Rogero
IPEN/CNEN-SP, Av. Prof. Lineu Prestes, 2242, CEP 05508-900, São Paulo, SP

Angelo Fernando Padilha
EPUSP, Av. Prof. Mello Moraes, 2463, CEP 05508-900 - São Paulo, SP – padilha@usp.br

Isolda Costa
IPEN/CNEN-SP, Av. Prof. Lineu Prestes, 2242, CEP 05508-900, São Paulo, SP - icosta@ipen.br

Abstract

In this study, the *in vitro* corrosion resistance of a superferritic stainless steel has been investigated in naturally aerated Hank's solution at 37°C by potentiodynamic polarization method and electrochemical impedance spectroscopy to evaluate its potential application as biomaterial. The polarization results have shown very low current densities at the corrosion potential and a behavior typical of passive metals. The polarization curve for the superferritic steel indicated a transpassive behaviour followed by a secondary passivation from potentials around 0.75 V(SCE) until potentials typical of the oxygen evolution reaction. The superferritic stainless steel showed high pitting resistance in the test solution and pitting was not found on the steel after polarization up to potentials of 3000 mV(SCE). The EIS results indicated high impedance values at low frequencies supporting the results from the polarization method. The results have been compared with that of Ti-13Nb-13Zr alloy, known as corrosion resistant and highly biocompatible alloy, under the same conditions. The corrosion rate determined from polarization curves is slightly higher for the superferritic stainless steel comparatively to the Ti-13Nb-13Zr alloy. Concerning the corrosion resistance the results indicated that the superferritic stainless steel could be considered a potential material for application as biomaterial. The cytotoxicity test showed no toxicity related to the superferritic steel by the agar diffusion methodology.

Keywords: impedance spectroscopy, superferritic stainless steel, alloy titanium, biomaterial, corrosion

1. Introduction

Stainless steels and titanium alloys are among the most used metallic materials for application as biomaterials. These materials present satisfactory mechanical properties and high corrosion resistance due to the adherent and protective oxide that forms spontaneously on their surfaces in various environments. The film formed is responsible for the passive behaviour found for these alloys. Such characteristics associated to biocompatibility are the required properties for biomaterials, considering that the body fluids are oxygenated saline solutions containing chloride and therefore highly corrosive. The biomaterials when in use are under mechanical strain solicitation, mainly when used as orthopedic and dental implants.

Titanium alloys have been extensively used as biomaterials and one of these alloys lately used is the Ti-13Nb-13Zr, that contains three of the four elements (Ti, Nb, Zr e Ta), that are related to excellent biocompatibility (Okazaki, 1999). Niobium is mainly used for β phase stabilization (Khan, 1999).

The AISI 316L is the most used stainless steel for surgical implants, mainly due to its low cost and high corrosion resistance (Sivakumar, 1993 and Pan, 1997). However, it has been reported that more than 90% of the implants fabricated with this type of steel corrode and, occasionally, localized corrosion, such as pitting and crevice corrosion, are seen on the surface of the implants removed from patients (Pan, 2000 and Nielson, 1987).

Corrosion and wear usually result in removal of metallic fragments or ions from the implant that are liberated into the tissues adjacent to it and causing the premature failure of the implant or adverse reactions that lead to implant's rejection (González, 1999). These observations have encouraged the search for new kinds of stainless steels that could be used as biomaterials. A superferritic stainless steel, with chromium contents above 25% and molybdenum content around 2.5%, are expected to present improved corrosion resistance comparatively to the AISI 316L steel, making it a more proper material for application as biomaterial. The literature on the characterization of this steel as biomaterials however is too scarce. The aim of this study was to evaluate the *in vitro* corrosion behaviour of a superferritic stainless steel in an artificial physiological solution (Hank's solution) naturally aerated and at 37°C, by means of electrochemical techniques aiming at its application as biomaterial. The results were compared with those of a Ti-13Nb-13Zr alloy, known as highly resistant to corrosion and biocompatible.

2. Experimental

In this study, a near-β Ti-13Nb-13Zr alloy and a superferritic stainless steel DIN X 1 CrNiMoNb 28 4 2 (Werkstoff-Nr. 1.4575) have been investigated. The Ti-13Nb-13Zr alloy was obtained by melting pure Ti and Nb (99.9%) and Zr containing up to 4.5% of Hf, in an arc melting furnace, using a non consumable electrode, in an argon atmosphere. After melting, the ingot was heat treated for 1 hour at 1000°C, followed by water-cooling, for homogenization. Subsequently, the alloy was cold worked (forged) until a diameter of 6.5 mm. During the stage of forging the alloy was once again heat treated at 1000°C, followed by water cooling (Schneider, 2001).

The chemical composition of the superferritic steel tested is shown in Tab (1). The steel was heat treated at 475ºC for 10 hours for precipitation of the α'phase. It is well known that such a heat treatment enhances the corrosion tendency. This treatment was performed in order to test the steel under such an adverse condition.

Table 1. Chemical composition (Weight %) of superferritic stainless steel DIN X 1 CrNiMoNb 28 4 2 (Werkstoff-Nr. 1.4575)

C	Si	Mn	P	S	Cr	W	Mo	V	Ni	Co	Nb	Ti	Cu	N	Fe
0.01	0.35	0.22	0.014	0.003	28.12	0.02	2.44	0.05	3.91	0.02	0.31	0.01	0.04	0.011	(64.34)

Electrodes were prepared by epoxy cold resin mounting of both alloys, leaving areas corresponding to 0.33 cm^2 and 0.25 cm^2, for the Ti alloy and the superferritic steel, respectively, for exposure to the electrolyte. The surfaces exposed to the electrolyte were prepared by sequential grinding with silicon carbide paper up to #2000 finishing, followed by mechanical polishing with diamond paste of 1 μm. After polishing the surface was rinsed in deionized water using an ultrasonic bath. After surface preparation and prior to EIS tests, all the samples remained immersed for 72 hours in Hank's solution, naturally aerated at 37°C, and the open circuit potential was measured until a steady state was reached, the corrosion potential (E_{corr}). The open circuit potential and its variation with time were measured since the first minutes of immersion.

A three-electrode cell arrangement was used, with a saturated calomel reference electrode (SCE) as reference electrode and a platinum wire as the auxiliary electrode. The polarization and EIS tests were carried out in triplicate. The electrolyte used to simulate the physiological medium was a Hank's solution whose composition is presented in Tab. (2). The electrochemical cells were sterilised in autoclave at 121°C to avoid bacteriological contamination of Hank's solution. The temperature of test (37°C) was controlled by a thermostatic bath, where the electrochemical cells were immersed for all test period.

Table 2. Chemical composition of Hank's solution.

Component	Concentration (Mol/L)
NaCl	0.1369
KCl	0.0054
$MgSO_4.7H_2O$	0.0008
$CaCl_2.2H_2O$	0.0013
$Na_2HPO_4.2H_2O$	0.0003
KH_2PO_4	0.0004
$C_6H_{12}O_6H_2O$	0.0050
Red phenol 1%	0.0071
pH	6.8

Polarization was carried out using a EG&G PARC 273A Potentiostat in the potential range from –800 mV(SCE) to 3000 mV(SCE) and the scan rate was 1mV/s. EIS tests were carried out by means of a Solartron SI-1255 coupled to a EG&G PARC 273A potentiostat and controlled by a software (Zplot). EIS measurements were obtained potentiostatically at the corrosion potential (E_{corr}) in the range from 100 kHz to 10 mHz, applying a 10 mV voltage amplitude and obtaining 6 points per decade.

The cytotoxicity test was carried out according to agar diffusion methodology, described elsewhere (Rogero, 2003). The specimen with dimensions of 0.5 x 0.5cm was laid on top of an agar layer above a monolayer cell culture in Petri's dish. Cell line of connective tissue of mice, NCTC Clone L-929 from American Type Culture Collection (ATCC) was used..

Latex fragment was used as positive control and atoxic filter paper disc as negative control. maintaining the surface area required by this methodology. The Petri's dishes were kept in humid incubator with 5% CO_2 atmosphere at 37°C for 24h. After this period the dishes were examined macroscopically and microscopically and the evaluation of

cytotoxicity was carried out by the presence of a halo around tested material and the size of the halo was measured with a millimetric ruler.

3. Results

Figure (1) shows the open circuit potential variation with time for both tested materials, superferritic steel and the Ti-13Nb-13Zr alloy in Hank's solution at 37°C. In the first minutes after immersion the potential of the superferritic steel was approximately –172 mV(SCE), and it rapidly increased to nobler potentials, reaching values around 100 mV (SCE) after 20 hours of immersion. The potential was fairly steady from 20 hours onwards, and after 56 hours its value was approximately 105 mV(SCE).

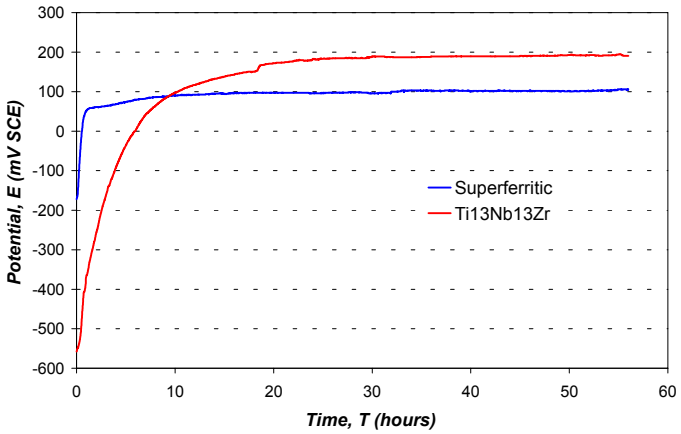

Figure 1. Corrosion potential variation with time curves for the superferritic steel and Ti-13Nb-13Zr alloy in Hank's solution at 37°C.

For the Ti-13Nb-13Zr alloy the initial potential, after immersion, was –558 mV (SCE), and after 24 hours it was fairly stable at 180 mV(SCE). The potential increased slowly from 24 hours to 56 hours, and after that period it was 192 mV(SCE)

Figure (2) shows the potentiodynamic polarization curves for the superferritic steel and the Ti-13Nb-13Zr alloy after 72 hours in Hank's solution at 37°C. The corrosion potential, E_{corr}, estimated from these curves for the superferritic steel and the Ti-13Nb-13Zr alloy were –464 mV (SCE) and –391 mV (SCE), respectively. The corrosion current densities (i_{corr}) were obtained from the polarization curves by extrapolation of the cathodic curve to the corrosion potential, and the results are shown in Tab. (3). The low values obtained are typical of a passive behaviour. The low i_{corr} values obtained are typical of passive materials. The current density in the passive region (i_{pp}), for the titanium alloy was approximately 4 μAcm^{-2} up to potentials of 900 mV(SCE). At potentials around 1260 mV(SCE) the current density increased to 16 μAcm^{-2}, suggesting transpassivation. However, the current density value did not change significantly until 3000 mV (SCE) showing that this alloy shows a secondary passivation.

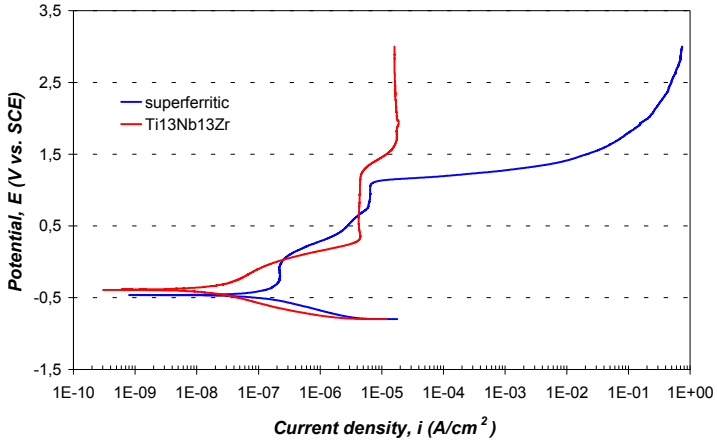

Figure 2. Potentiodynamic polarization curves for Ti-13Nb-13Zr alloy and superferritic steel after 72 hours of immersion in Hank's solution at 37°C.

The superferritic alloy has a behaviour slightly different, showing a i_{pp} around 0,2 μAcm^{-2}, in the range from –230 mV (SCE) to 40 mV (SCE). As the potential increased from 40 mV (SCE) there was a direct dependence between the potential and the current, the current increasing as the potential increased. From 1120 mV (SCE) onwards the current

variation with potential was typical of transpassivation, likely due to oxygen evolution. Another possible reason for the increase in current at potentials above 1120 mV (SCE) could be pitting. However, pitting was not seen on the titanium alloy surface after polarization test , as Fig. (3) shows.

Table 3. Corrosion potential and corrosion current density values in Hank's solution for the Ti-13Nb-13Zr alloy and superferritic steel.

Ti-13Nb-13Zr		**Superferritic steel**	
E_{corr} mV(SCE)	i_{corr} nA/cm^2	E_{corr} mV(SCE)	i_{corr} nA/cm^2
-409 (43)	30 (16)	-483 (28)	196 (65)

(*) entries are mean (standard deviation) N=4

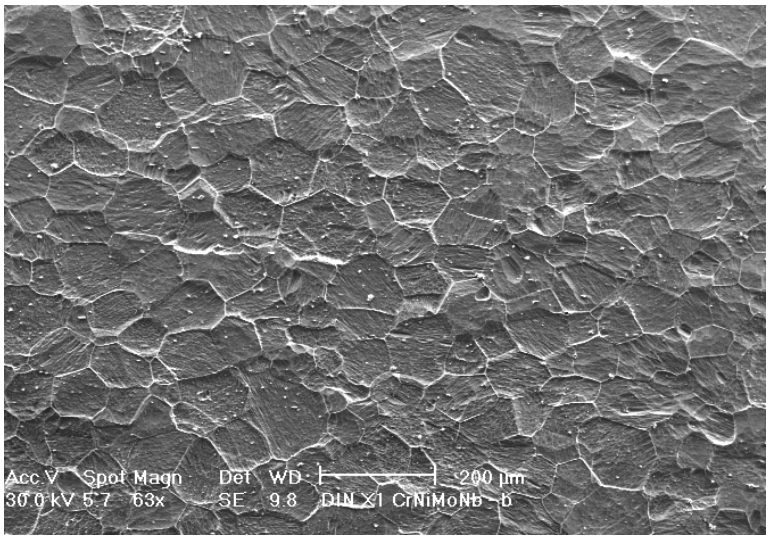

Figure 3. Micrography of superferritic steel after polarization up to 3000 mV (SCE) in Hank's solution at 37°C.

Figure (4) shows Bode diagrams (phase angle and Z) for the superferritic steel and for the Ti-13Nb-13Zr alloy, at the corrosion potential at 72 hours of immersion in Hank's solution at 37°C. The phase angle diagram indicates a highly capacitive behaviour, typical of passive materials, with phase angles approaching –90 degrees from intermediate to low frequencies. This result suggests a passive film of high stability in the test solution.

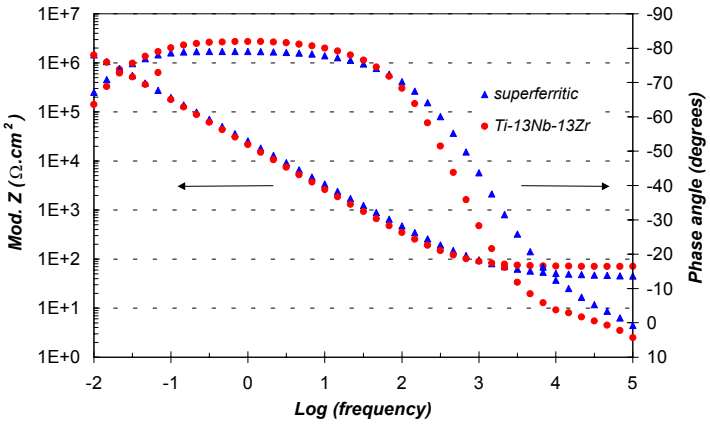

Figure 4. Bode diagrams (phase angle vs. log f and Z modulus vs. log f) for Ti-13Nb-13Zr alloy and superferritic steel after 72 hours of immersion in Hank's solution at 37°C.

The obtained spectra were interpreted in terms of an "equivalent circuit" with the circuit elements representing electrochemical properties of the alloy and its oxide film. Figure (5) shows the equivalent circuit used for fitting the spectra obtained for the Ti-13Nb-13Zr alloy, which was proposed by Mansfeld and Kendig (Mansfeld, 1988) for

anodized aluminium. R_b and C_b represent the resistance and capacitance of the barrier layer, and R_p and C_p, represent the resistance of the porous layer with the electrolyte inside the pores and capacitance of the porous layer, respectively.

Figure (6) shows the equivalent circuit used for fitting the spectra obtained for the superferritic steel. R_{pass} and C_{pass} represent the resistance and capacitance of the passive film on the steel. The quality of fitting to the equivalent circuit was judged by the chi-squared values. The results of this fitting are presented in Tab. (4) and Tab. (5) for Ti-13Nb-13Zr and superferritic steel, respectively. The obtained values of chi-squared (order of 10^{-3}) indicate a good fitting to the proposed circuit.

Despite of a constant phase element (CPE) being utilised for data fitting instead of an ideal capacitor, for simplicity reasons, the value obtained from data fitting was taken as the capacitance.

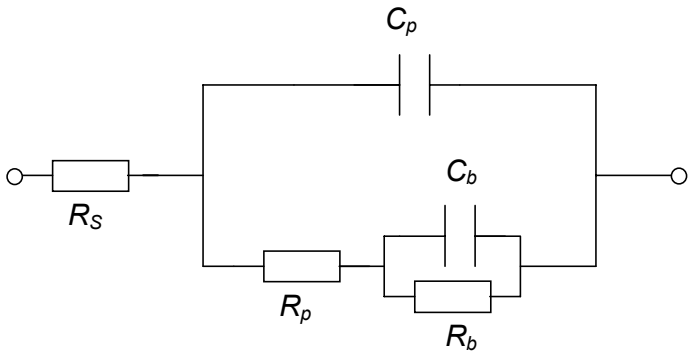

Figure 5. Equivalent circuit for fittingexperimental data of Ti-13Nb-13Zr alloy in Hank's solution at 37°C.

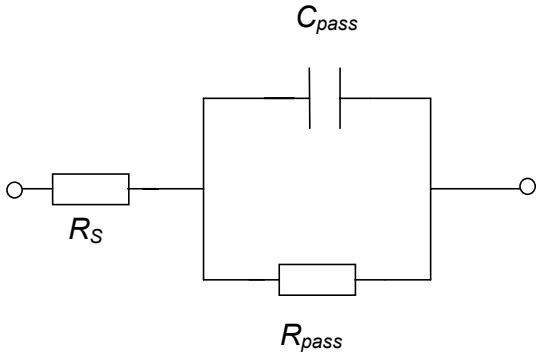

Figure 6. Equivalent circuit for fitting experimental data of superferritic steel in Hank's solution at 37°C.

The impedance of a constant phase element is given by $Z_{CPE} = [C(jw)^n]^{-1}$, where $-1 \le n \le 1$. The n value is related to irregular distribution of current due to rugosity and/or defects on the surface. For the Ti-13Nb-13Zr alloy, the n values corresponding to the porous and barrier layer were 0,90 and 0,89, respectively and for the superferritic steel, n was approximately 0,89. The barrier layer is a compact and thinner layer and the n values close to 1 indicates that it approaches the bevahior of an ideal capacitor (Gonzales, 1999).

Table 4. Resistance and capacitance values related to the oxide layer in Ti-13Nb-13Zr. Values estimated by fitting the data to the equivalent circuit in Fig. (5).

	R_s ($\Omega.cm^2$)	C_p (μFcm^{-2})	R_p ($\Omega.cm^2$)	C_b (μFcm^{-2})	R_b ($\Omega.cm^2$)	Chi-squared
Ti-13Nb-13Zr	141	8	1636	1,3	4.6E6	1.7E-3

Table 5. Resistance and capacitance values related to the oxide layer in superferritic steel. Values estimated by fitting the data to the equivalent circuit in Fig. (6).

	R_s ($\Omega.cm^2$)	C_{pass} (μFcm^{-2})	R_{pass} ($\Omega.cm^2$)	Chi-squared
Superferritic steel	66	6	1.5E7	5.7E-3

The results of cytotoxicity test showed that only the positive control (latex fragment) produced a halo of 21 mm diameter around the sample. The negative control did not present any halo and the cells around the sample showed neither injury nor morphological modifications. The superferritic steel showed a behaviour similar to that of the negative control. The positive and negative controls are used for evaluating the performance of the methodology adopted. Based on the obtained results it can be concluded that the superferritic steel presented no cytotoxicity in the agar diffusion methodology.

3. Discussion

The corrosion potential variation with time curves, shown in Fig. (1), are typical of passive metals immersed in aerated solutions. The corrosion potential of these metals is defined by the intersection of the passive anodic curve with the cathodic curve of oxygen reduction reaction in the range where it displays activation polarization behaviour. As the time increases, the passive film usually becomes more protective, likely due to film thickening, so that the passive current density (i_{pass}) tends to decrease. Consequently, the intersection of the passive straight line with the cathodic curve is shifted to higher potentials. Thus, the corrosion potential increases until the passive film reaches its limiting protective capacity resulting in stabilization of the corrosion potential (Lavos-Valereto, 2002).

The corrosion potentials obtained from potentiodynamic polarization curves, Fig. (2) are much lower than those shown in Fig. (1) and this was likely due to the polarization tests have started at cathodic potentials about 900 mV to 1000 mV below the corrosion potential. The passive film, present at the surface of both samples, was probably removed because of the highly reducing initial potentials (Lavos-Valereto, 2002).

The two polarization curves are typical of a direct transition from the immunity region to the passive region. The corrosion potential in these curves is defined by the intersection of the activation polarization anodic curve related to the formation of passive film with the activation cathodic curve of oxygen reduction reaction. This intersection takes place in lower potentials than when there is already a well-formed passive film on the surface (Lavos-Valereto, 2002).

The equivalent circuit illustrated in Fig. (5) was proposed by Mansfeld and Kendig [11] to describe the bilayer oxide formed on porous aluminium oxide films. This circuit was also proposed in the literature to represent the oxide film on Ti-6Al-4V (Venugopalan, 2000). According to the literature (Hefny, 1982 and EL-Basiouny, 1982), there is substantial evidence that the film formed on titanium in aqueous solutions, in many exposure conditions, exhibits a two layer structure composed of a dense inner layer and a porous outer layer. It has been found that the titanium oxide is essentially TiO_2, with a transient region between the inner and the outer layers (Pan, 1997).

The two-layer model of the oxide film related to the titanium alloy was well supported by EIS results obtained in this study. Large values of R_b at E_{corr} (order of 10^6 $\Omega.cm^2$) were obtained supporting the passivation of the Ti-13Nb-13Zr alloy in Hank's solution. R_b was much greater than R_p, showing that the resistance of the oxide film is mainly due to this layer. An investigation with a commercial Ti-6Al-7Nb alloy in Hank's naturally aerated solution at 25°C also produced similar results (Lavos-Valereto, 2003).

A two layer model was not appropriate for adjusting the EIS data of the superferritic steel. The results indicate that the passive film is formed by a unique layer, and the value of the resistance (R_{pass}) related to this layer was of the order of 10^7 $\Omega.cm^2$. The high resistance of the passive film and its low capacities (a few μFcm^{-2}), as shown in Tab. (5), support a highly resistant material (passive behaviour) as indicated by the results of the other electrochemical techniques used. The phase angles approaching –90 degrees from intermediate to low frequencies is characteristic of a compact passive film (González, 1999).

A comparison of the results for the titanium alloy investigated with those for the superferritic steel shows that the results of the three electrochemical techniques were compatible. The corrosion potential variation with time curves indicate a slightly nobler potential related to the titanium alloy comparatively to that of the superferritic steel. The corrosion current densities and corrosion potentials obtained from potentiodynamic polarization curves for the titanium alloy were also lower than those for the superferritic steel. The EIS data support the results from the other techniques showing a more capacitive behaviour related to the titanium alloy than that for the superferritic steel. Despite of the increased corrosion resistance of the titanium alloy comparatively to the superferritic steel tested, it is important to emphasize that the corrosion resistance of the superferritic steel was excellent and only slightly inferior to that of the Ti-13Nb-13Zr alloy.

4. Conclusions

- The electrochemical results indicated a passive behaviour for both tested materials (Ti-13Nb-13Zr alloy and superferritic stainless steel) in naturally aerated Hank's solution at 37°C. The corrosion current densities were of the order of 10^{-1} μAcm^{-2} (superferritic steel) and 10^{-2} $\mu A.cm^{-2}$ (Ti-13Nb-13Zr), suggesting a highly resistant passive film.

- The cytotoxicity test showed no toxicity related to the superferritic steel by the agar diffusion methodology. The large resistances related to the films formed on both tested alloys and their highly capacitive behaviour in a large range of frequencies also show that the oxide films on their surfaces are highly resistant to corrosion.

- The electrochemical and cytotoxicity results of the superferritic steel in the simulated physiological solution at 37°C, which were comparable to that of the Ti-13Nb-13Zr alloy, known as highly corrosion resistant and biocompatible alloy, indicated that the superferritic stainless steel must be considered a potential material for application as biomaterial.

6. Acknowledgements

The authors are grateful to S. Schneider for providing the Ti-13Nb-13Zr alloy used in this investigation.

7. References

EL-Basiouny, M.S. and Mazhar, A. A.; Electrochemical behavior of passive layers on titanium; Corrosion, 38(5):237-240, 1982.

González, J. E. G. and Mirza-Rosca, J. C.; Study of the corrosion behavior of titanium of its alloys for biomedical and dental implant applications; Journal of Electroanalytical Chemistry, v. 471, pp.109-115, 1999.

Hefny, M.M.; Mazhar, A.A.; EL-Basiouny, M. S.; Dissolution behaviour of titanium oxide in H_2SO_4 and NaOH from impedance and potential measurements; British Corrosion Journal, v. 17, n. 1, 38-41, 1982.

Khan, M. A.; Williams, R. L. and Williams, D. F.; The corrosion behavior of Ti6Al4V, Ti6Al7Nb and Ti-13Nb-13Zr in protein solutions; Biomaterials, v. 20, pp. 631-637, 1999.

Lavos-Valereto, I. C.; Costa, I.; Wolynec, S.; The electrochemical behavior of Ti6Al7Nb alloy with and without plasma-sprayed hydroxyapatite coating in Hank's solution; Journal of Biomedical Materials Research; v. 63 (5), pp. 664-670, 2002.

Lavos-Valereto, I. C.,;Ramires, I.; Guastaldi, A.C.; Costa, I.; Wolynec, S.; Electrochemical impedance spectroscopy of Ti-6Al-4V alloy for dental implant in Hank's solution. Submitted to Hournal of Materials Science: Materials in Medicine, 1993.

Mansfeld, F. and Kendig, M.W.; Evaluation of anodized aluminum surfaces with electrochemical impedance spectroscopy. Journal Electrochemical Society, 135(4), 828-833, 1988.

Nielsen, K.; Corrosion of metallic implants; British Corrosion Journal, v. 22, n. 4, 272-278, 1987.

Okazaki, Y.; Ito, Y.; Kyo, K. and Tateishi, T.; Corrosion resistance and corrosion fatigue strength of new titanium alloys for medical implants without V and Al; Materials Science and Engineering A, v.213, 138-147, 1996.

Pan, J.; Karlen, C.; Ulfvin, C.; Electrochemical study of resistance to localized corrosion of stainless steels for biomaterial applications; Journal of Electrochemical Society, 147, (3), 1021-1025, 2000.

Pan, J.; Thierry, D.; Leygraf, C and Ektessabi, A. M.; Corrosion resistance for biomaterial applications of TiO_2 films deposited on titanium and stainless steel by ion-beam-assisted sputtering; Journal of Biomedical Materials Research, v. 35, pp. 309-318, 1997.

Rogero, S.O.; Lugão, A.B.; Ikeda, T.I.; Cruz, A.S.; In vitro cytotoxicity test: A comparative study of two methodologies.; Material Research, v.6, n. 2, 2003, (In portuguese).

Schneider, S. G.; Obtenção e caracterização da liga Ti-13Nb-13Zr para aplicação como biomaterial; São Paulo: 2001, Tese (Doutoramento) - Instituto de Pesquisas Energéticas e Nucleares.

Sivakumar, M.; Kamachi Mudali, U.; Rajeswari, S.; Compatibility of ferritic and duplex stainless steels as implant materials: in vitro corrosion performance; Journal of Materials Science, 28, pp. 6081-6086, 1993.

Venugopalan, R.; Weimer, J. J.; George, M. A.; Lucas, L. C.; The effect of nitrogen diffusion hardening on the surface chemistry and scratch resistance of Ti-6Al-4V alloy; Biomaterials, 21, 1669-1677, 2000.